Fragmentation and Emergent Integrable Transport in the Weakly Tilted Ising Chain

Alvise Bastianello,[1,2,3] Umberto Borla,[1,3] and Sergej Moroz[1,3,4]
[1]Department of Physics, Technical University of Munich, 85748 Garching, Germany
[2]Institute for Advanced Study, 85748 Garching, Germany
[3]Munich Center for Quantum Science and Technology (MCQST), Schellingstr. 4, D-80799 München, Germany
[4]Department of Engineering and Physics, Karlstad University, Karlstad 651 88, Sweden

(Received 8 September 2021; accepted 7 April 2022; published 11 May 2022)

We investigate emergent quantum dynamics of the tilted Ising chain in the regime of a weak transverse field. Within the leading order perturbation theory, the Hilbert space is fragmented into exponentially many decoupled sectors. We find that the sector made of isolated magnons is integrable with dynamics being governed by a constrained version of the XXZ spin Hamiltonian. As a consequence, when initiated in this sector, the Ising chain exhibits ballistic transport on unexpectedly long timescales. We quantitatively describe its rich phenomenology employing exact integrable techniques such as generalized hydrodynamics. Finally, we initiate studies of integrability-breaking magnon clusters whose leading-order transport is activated by scattering with surrounding isolated magnons.

DOI: 10.1103/PhysRevLett.128.196601

Introduction.—The celebrated Ising model contributed to several paradigm shifts in physics. In classical statistical mechanics, Onsager's solution [1] on a two-dimensional lattice kick-started the development of a general theory of continuous phase transitions. It is well known that in the presence of a transverse field only, the one-dimensional quantum Ising chain is exactly solvable [2–4] and reduces via the Jordan-Wigner transformation to a free Majorana chain [5]. On the other hand, the addition of a longitudinal field breaks the integrability of the model. In the ferromagnetic case, this leads to confinement of fermionic domain walls into bosonic magnons [6–9]. Recent studies concentrated on aspects of anomalously slow dynamics [10–15], quantum scarring [16,17], prethermalization [18], fractons [19], meson scattering [20,21], dynamics of the false vacuum [22–27], and emergent $\mathbb{Z}_2$ lattice gauge theories [28,29].

In this Letter, we unveil unexpected features of the one-dimensional quantum Ising model in a weakly tilted field. Specifically, we investigate transport in the prototypical partitioning protocol [30]: the chain is initialized into two halves which are then connected, activating transport across the junction. We observe strong signatures of ballistic behavior for unexpectedly long times in the regime where the transverse field is small. Moreover, we discover that the nature of transport exhibits a strong dependence on the longitudinal field and on the Ising coupling. Using degenerate perturbation theory as a tool, we argue that the effective Hamiltonian in this regime enjoys two separate U(1) conservation laws for the number of magnons and domain walls. These two symmetries are emergent as they are not imprinted in the microscopic Hamiltonian. We show that, at leading order in perturbation theory, the effective dynamics fragments the Hilbert space (expressed in the canonical local basis) into a large number of independent sectors that scales exponentially in the system size. Among all sectors we first focus on the dynamics of isolated magnons, which we find to be integrable. This finding accounts for the emergence of ballistic behavior—a clear signature of integrability—in contrast to the naively expected diffusion. Specifically, this sector is governed by the constrained XXZ Hamiltonian first investigated by Alcaraz and Bariev [31] with coordinate Bethe Ansatz. Apart from early studies [32,33] this model went unnoticed for a long time, but recently appeared in several independent contexts, e.g., in the constrained PXXP model [34], in the strongly coupled regime of a $\mathbb{Z}_2$ lattice gauge theory coupled to fermions [35], and in interacting correlated hopping models [36]. At the noninteracting point, that is nontrivial due to the constraint, it emerges in the strong coupling limit of the canonical XXZ spin chain [37–39]. The leitmotif of some of these studies is the phenomenon of Hilbert space fragmentation [40–44] due to imposed or emergent constraints which make the constrained XXZ chain a natural candidate to describe integrable sectors, if present. Moreover, see also Refs. [45–47] for related integrable constrained models with medium range interactions. Using generalized hydrodynamics (GHD) [48,49] (see also Refs. [50–56]) we analytically tackle transport within the isolated magnon sector. The Alcaraz-Bariev (AB) model inherits the rich phenomenology of the XXZ spin chain: transport greatly depends on the interactions and can exhibit sharp jumps [57]. We find that the hydrodynamics of the AB model is peculiar on its own, since in certain regimes of interactions quasiparticles carry fractional magnetization, in clear contrast with the

vast majority of integrable models and signaling the collective nature of the excitations. The presence of two or more neighboring magnons breaks integrability and probes the transport of surrounding isolated magnons. Indeed, within the leading order perturbation theory clusters of magnons are completely immobile in isolation, but we show they undergo magnon-assisted hopping experiencing biased diffusion, whose mean and variance are directly connected to the magnetization current crossing them.

Emergent ballistic transport in the Ising chain in a weak transverse field.—With the help of time evolving block decimation (TEBD) [58], we start by numerically investigating transport in the Ising chain in a tilted magnetic field

$$H = -J\sum_i Z_i Z_{i+1} - h_\parallel \sum_i Z_i - h_\perp \sum_i X_i, \qquad (1)$$

where X_i and Z_i denote the Pauli matrices at site i. In the partitioning protocol [30], one initializes the state in two different halves $|\Psi\rangle = |\Psi_L\rangle \otimes |\Psi_R\rangle$ and then lets the system evolve with the homogeneous Hamiltonian. In Fig. 1(a) we choose $|\Psi_L\rangle$ and $|\Psi_R\rangle$ to be the Neel and ferromagnetic state respectively, and we focus on the regime where the transverse field is weak. While the Hamiltonian [Eq. (1)] is known to be nonintegrable for generic values of the parameters, our analysis unveils persistent ballistic transport typical of integrable models [48,49], in contrast with the naively expected diffusion. With this choice of initial states, we also observe a strong dependence of transport on the longitudinal field and the Ising coupling with a light cone suppression whenever $0 < h_\parallel/J < 4$; see Fig. 1(b). This

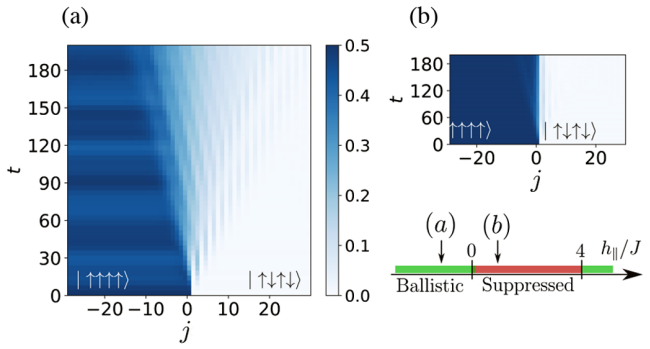

FIG. 1. Magnetization profiles $\langle S_j^z \rangle$ in the Ising chain at $J = 1$ and $h_\perp = 0.2$ initialized by joining the ferromagnetic and Neel states. (a) For $h_\parallel = -0.7$ we observe ballistic transport with a characteristic light cone. (b) For $h_\parallel = 0.7$ we find strong suppression of spin transport. TEBD simulations are done for a chain of length $L = 80$. The peculiar transport is captured by the integrable dynamics governed by the Hamiltonian [Eq. (3)] which emerges for a weak transverse field $h_\perp \ll h_\parallel, J$. The validity of the phase diagram is within this limit; see main text for discussion.

unexpected behavior can be ascribed to a peculiar integrable model, as we now discuss.

Effective Hamiltonian.—We analyze the Ising chain [Eq. (1)] in the regime where the transverse field $h_\perp$ is much smaller than the two generic (but incommensurate) couplings J and $h_\parallel$. To set up a perturbative expansion we split the Hamiltonian [Eq. (1)] into the classical Z-dependent part H_0 (the Ising and longitudinal field terms) and the transverse field perturbation. Since $[H_0, Z_i] = 0$, the Hamiltonian H_0 has an extensive number of symmetries and trivially splits in the Z basis into 2^L independent blocks. Notwithstanding, its energy spectrum is organized into degenerate multiplets characterized only by a pair of emergent U(1) quantum charges: the magnon number N and the domain wall number $D = \sum_i (1 - Z_i Z_{i+1})/2$. By construction, N and D are both simultaneously preserved by the effective perturbative dynamics. The transverse field perturbation changes the number of magnons and thus can contribute only at even orders of the degenerate perturbation theory. Employing the Schrieffer-Wolff transformation [59,60], in the Supplemental Material [61] we have constructed the second-order effective perturbative Hamiltonian

$$H_{\text{eff}}^{(2)} = -\sum_{s=\pm 1} t_s \sum_j \mathcal{P}^s_{j-1,j+2} (S_j^+ S_{j+1}^- + \text{H.c.}) - g\sum_j Z_{j-1} Z_j Z_{j+1} - \delta J \sum_j Z_j Z_{j+1} - \delta h_\parallel \sum_j Z_j, \qquad (2)$$

where the spin-exchange coupling $t_s = h_\perp^2 h_\parallel^{-1} J/(h_\parallel + 2sJ)$, the projector $\mathcal{P}^s_{i,j} = [1 + s(Z_i + Z_j) + Z_i Z_j]/4$, and $S_j^\pm = (X_j \pm iY_j)/2$. Moreover, the induced three-spin coupling $g = h_\perp^2 h_\parallel^{-1} J^2/\alpha$ and the shifts of the Ising and longitudinal couplings are $\delta J = -h_\perp^2 J/\alpha$ and $\delta h_\parallel = h_\perp^2 h_\parallel^{-1}(h_\parallel^2 - 2J^2)/(2\alpha)$, where we introduced $\alpha = h_\parallel^2 - 4J^2$. Corrections beyond Eq. (2) are $\mathcal{O}(h_\perp^4)$ and are discussed in the Supplemental Material [61]. The Hamiltonian agrees with the previous derivation [62]; see also Refs. [21,36] for related studies. Domain wall conservation enforces the projector $\mathcal{P}^s_{i,j}$ ensuring that the two outer spins surrounding the exchange pair point in the same direction. A similar type of hopping has been recently discussed in Refs. [36–39]. Since only isolated magnons can hop, the perturbative model [Eq. (2)] supports a large number of immobile (frozen) quantum states that contain clusters of magnons.

The number F_l of independent frozen states of size $l \gg 1$ scales exponentially $F_l \sim \varphi^l$, where φ is the golden ratio [36]. In the Supplemental Material [61] we demonstrate that for chains of size $L \gg 1$ the effective Hamiltonian [Eq. (2)] splits into φ^{L+1} independent blocks. Such exponential growth is parametrically larger than the $O(L^2)$ scaling expected purely from the two U(1) emergent symmetries. A similar pattern of fragmentation of the Hilbert space was discovered in spin models in the strict confinement regime

[36]. Consider first a sector with N isolated spin-down sites in the spin-up background. In this case $D = 2N$ and pairs of magnons cannot appear next to each other. In this sector the second-order Hamiltonian [Eq. (2)] reduces to

$$H_{\text{eff}}^{(2)} \to -\mathcal{J}\sum_j \mathcal{P}_1(S_j^x S_{j+1}^x + S_j^y S_{j+1}^y + \Delta S_j^z S_{j+2}^z)\mathcal{P}_1, \quad (3)$$

where the projector $\mathcal{P}_1$ prohibits two spin-down magnons from occupying neighboring sites. The inverse of the coupling $\mathcal{J} = 2t_+$ defines the slow timescale associated with hopping of the isolated magnons. The anisotropy parameter $\Delta = 2J/(h_\parallel - 2J)$ can be tuned by changing the dimensionless ratio $h_\parallel/J$. This model is a constrained version of the celebrated XXZ chain which was first investigated by Alcaraz and Bariev [31]. Remarkably, the Hamiltonian [Eq. (3)] at $\Delta = 1/2$ is known to be a supersymmetric model [63,64], which can be realized in a Rydberg-based quantum simulator [65].

Transport in the Alcaraz-Bariev model.—The AB model can be generalized to the extended hard-core constraint $\mathcal{P}_1 \to \mathcal{P}_T$ prohibiting magnons closer than T sites. The original papers [31–33] addressed the equilibrium thermodynamics. For $\Delta = 0$ and $T = 1$, the AB model governs the isolated magnon sector of the folded XXZ spin chain [37–39]. Here we focus on transport and hydrodynamics of the AB model at arbitrary Δ.

Being integrable, the AB model possesses an extensive number of (quasi-)local conserved quantities [66], with striking consequences on its nonequilibrium features, hindering thermalization [67] and featuring ballistic transport [51]. The AB Hilbert space is made of multiparticle magnonic asymptotic states labeled by the set of rapidities $\{\lambda_j\}_{j=1}^N$, which generalize the momenta of noninteracting systems. Because of integrability, multiparticle scattering events can be factorized in two-body scattering processes, the latter fully described by the scattering phase $\Theta(\lambda, \lambda')$. The scattering phase of the AB model and of the XXZ spin chain are connected [31,61] $\Theta(\lambda, \lambda') = Tp(\lambda) - Tp(\lambda') + \Theta^{XXZ}(\lambda - \lambda')$, with $p(\lambda)$ the momentum of the magnon. The relation resembles the celebrated $T\bar{T}$ deformation; see Refs. [68–74] and references therein. On a finite chain, the allowed rapidities are quantized, similarly to the momenta of noninteracting models. However, the interactions couple the rapidities through the highly nonlinear Bethe equations [61,75], which explicitly depend on Θ. Being nonlinear, the Bethe equations are difficult to solve. In the zero density limit ($L \to \infty$, N fixed), the solutions of the Bethe equations form groups of rapidities sharing the same real part, but shifted in the imaginary direction. These special solutions are called strings and are determined by the zeroes and poles of the scattering matrix $e^{i\Theta(\lambda,\lambda')}$ [75] and are readily interpreted as bound states of magnons. Since the factor $e^{iT[p(\lambda)-p(\lambda')]}$ does not have zeros or poles, in the AB scattering matrix these are entirely determined by the XXZ scattering matrix. Hence the two models share the same pattern of strings.

The string hypothesis [75] claims the persistence of strings even in the thermodynamic limit ($L \to \infty$, $N/L = n$ fixed). Within the thermodynamic Bethe ansatz (TBA) [75], one opts for a coarse-grained description of the Bethe equations, defining the so-called root densities $\rho_j(\lambda)$, one for each string, where λ parametrizes the (real) center of the string. Then, $L\mathrm{d}\lambda\rho_j(\lambda)$ is interpreted as the number of solutions of the jth string within the interval $[\lambda, \lambda + \mathrm{d}\lambda]$. The interactions affect the occupancy; hence, the need of introducing the total root density $\rho_j^t(\lambda) \geq \rho_j(\lambda)$ representing full occupancy (see the Supplemental Material for details [61]). The root densities fully determine the equilibrium thermodynamics and homogeneous nonequilibrium steady states [66,76,77]. Moreover, they are the building blocks of GHD. Since the AB and XXZ models are closely related, it is worth properly addressing the string hypothesis in the latter. The string classification in the XXZ chain is textbook material [75], and we summarize it in the Supplemental Material [61]. The structure of XXZ strings greatly depends on the parameter Δ: in particular, for $|\Delta| \geq 1$ the string hypothesis, strictly speaking, does not cover the entire phase space. The thermodynamics of the strings built on the all-spin-up reference state covers only states up to half filling $0 < n < 1/2$, with n being the density of flipped spins. In the XXZ model, one circumvents this limitation by using the reflection symmetry $S_j^z \to -S_j^z$ and building the string hypothesis on the symmetric all-spin-down reference state. The two descriptions together cover the whole phase space and, in addition to the root densities, one introduces the magnetization sign $\mathfrak{f} = \pm 1$ to specify the sector. In the case $|\Delta| < 1$, the string hypothesis covers all magnetization sectors, and $\mathfrak{f}$ is not needed.

In the AB model, the constraint shifts the half filling point to the value $1/(2 + T)$. Moreover, it breaks the spin reflection symmetry. In Ref. [31] the Bethe equations of the AB model in all sectors have been mapped onto the corresponding equations for the XXZ chain in a reduced magnetization-dependent volume. Building on these ideas, we now determine the thermodynamics of the AB model at a generic filling, which is described by the same set of root densities as the XXZ spin chain. Above half filling, these cannot be interpreted as strings anymore; however, for the sake of retaining a standard notation, we will still refer to these root densities as strings. In addition, for $|\Delta| > 1$ one needs an extra bit of information $\mathfrak{f} = \pm 1$ that distinguishes the regions below and above half filling, respectively. When addressing thermodynamics and transport, it is crucial to know the amount of magnetization carried by each string. Within the ordinary string hypothesis, this is simply the number of magnons belonging to the same bound state. In the XXZ case, one has $m_j^{XXZ} = \mathfrak{f}|m_j^{XXZ}|$, with $|m_j^{XXZ}|$ a $\mathfrak{f}$-independent integer. On the other hand, in the AB model

we find an explicitly $\mathfrak{f}$-dependent magnetization $m_j = [1+T(1-\mathfrak{f})/2]^{-1} m_j^{XXZ}$. We observe that for $\mathfrak{f} = -1$ (needed if $|\Delta| > 1$) the string magnetization m_j becomes fractional! This signals the lack of microscopic interpretation of the root density as a bound state of magnons. We found that the nontrivial $\mathfrak{f}$ dependence extends from the magnetization to thermodynamic observables. To see that we consider the TBA string scattering phase $\Theta_{j,j'}(\lambda,\lambda')$ that, whenever the string hypothesis holds, is obtained from $\Theta(\lambda,\lambda')$ summing over the constituents of the string. In all sectors it can be written as

$$\Theta_{j,j'}(\lambda,\lambda') = T p_j(\lambda) m_{j'} - T m_j p_{j'}(\lambda') + \Theta^{XXZ}_{j,j'}(\lambda-\lambda'). \quad (4)$$

The appearance of the magnetization m_j makes $\Theta_{j,j'}$ explicitly $\mathfrak{f}$-dependent. In addition, we find that $\mathfrak{f}$ renormalizes the total root density $2\pi\sigma_j\rho_j^t = (\partial_\lambda p_j)^{\mathrm{dr}}[1+T(1-\mathfrak{f})/2]^{-1}$, where σ_j is the string parity and the standard definition of dressing is $(\partial_\lambda p_j)^{\mathrm{dr}} = \partial_\lambda p_j - \sum_{j'} \int [(d\lambda)/(2\pi)] \partial_\lambda \Theta_{j,j'}(\lambda,\lambda') \vartheta_{j'}(\lambda') \sigma_{j'} (\partial_{\lambda'} p_{j'})^{\mathrm{dr}}$, with $\vartheta_j = \rho_j/\rho_j^t$ being the filling fraction. With these caveats, one can recover the full equilibrium thermodynamics by standard methods: we leave the details to the Supplemental Material [61] and move on toward discussing hydrodynamics. Let us imagine that the system, still governed by the homogeneous AB Hamiltonian, features a long wavelength inhomogeneity in the state. In the limit of weak inhomogeneities, one can invoke local relaxation to (weakly) space-time dependent root densities. This is the idea behind GHD [48,49], which in its simplest form describes the convective expansion of particles $\partial_t \rho_j(\lambda) + \partial_x [v_j^{\mathrm{eff}}(\lambda)\rho_j(\lambda)] = 0$. The effective velocity

$$v_j^{\mathrm{eff}}(\lambda) = [\partial_\lambda \epsilon_j(\lambda)]^{\mathrm{dr}} / [2\pi\sigma_j \rho_j^t(\lambda)], \quad (5)$$

depends on the state due to interactions, making the equation nonlinear. Above, ϵ_j is the energy carried by the string. In contrast to the AB model, in most integrable systems the identity $2\pi\sigma_j\rho_j^t = (\partial_\lambda p_j)^{\mathrm{dr}}$ holds, leading to the alternative more intuitive definition $v_j^{\mathrm{eff}}(\lambda) = (\partial_\lambda \epsilon_j)^{\mathrm{dr}}/(\partial_\lambda p_j)^{\mathrm{dr}}$ that was originally reported in Refs. [48,49]. However, in a recent rigorous proof [55,78,79], Eq. (5) naturally emerges from the calculations. At a technical level, Eq. (5) arises in the AB model naturally by manipulating the hydrodynamic equations [61]. To the extent of our knowledge, this is the only model with this feature. In the case with $|\Delta| > 1$, the spin flip continuity $\partial_t n + \partial_x j_n = 0$, with $n = (1-\mathfrak{f})/[2+T(1-\mathfrak{f})]^{-1} + \sum_j \int \mathrm{d}\lambda m_j \rho_j(\lambda)$ and $j_n = \sum_j \int d\lambda v_j^{\mathrm{eff}}(\lambda) m_j \rho_j(\lambda)$, closes the hydrodynamic equations giving a further condition on $\mathfrak{f}$, similar to the XXZ model [57].

The partitioning protocol and GHD.—We now apply GHD of the AB model to the partitioning protocol. After a short transient the profile of local observables becomes scale invariant [48,49] $\langle \mathcal{O}(t,x)\rangle = F[x/t]$ and curves at a different time collapse when plotted as a function of the ray $\zeta = x/t$. As we show in Fig. 2(a), if one starts from an initial state with only isolated magnons the Ising chain agrees with the underlying AB description (up to a time-scale $t \sim h_\perp^{-4}$) and supports ballistic transport. Note that for $|\Delta| \geq 1$, i.e., $0 \leq h_\parallel/J \leq 4$, the magnetization sign $\mathfrak{f}$ is responsible for sharp jumps whenever states from the two different magnetization sectors are joined. At $t = 0$, the $\mathfrak{f}(x)$ profile is a step function and due to discreteness of $\mathfrak{f}$, GHD cannot smoothen its profile, but only moves the position of the jump. The explicit $\mathfrak{f}$-dependence of the TBA induces nonanalyticities not only in the magnetization profile (as in the XXZ chain [57]), but in all conserved charges.

An extreme example is presented in Fig. 1: for $|\Delta| \geq 1$, the Neel state and the ferromagnetic states have the exactly same trivial root density $\rho_j(\lambda) = 0$, but differ in the sign of $\mathfrak{f}$ [61]. Hence, any smooth dependence of the profile is suppressed and only the jump, that is pinned at the origin, remains. In this case, transport is inhibited. Whenever the initial root density of the two halves is known, GHD provides an exact solution of the partitioning protocol; see Fig. 2 and the Supplemental Material [61] for further evidence.

Beyond isolated magnons.—Sectors which contain frozen clusters of magnons appear to be generically not integrable: their energy level statistics [80,81] falls into the class of the

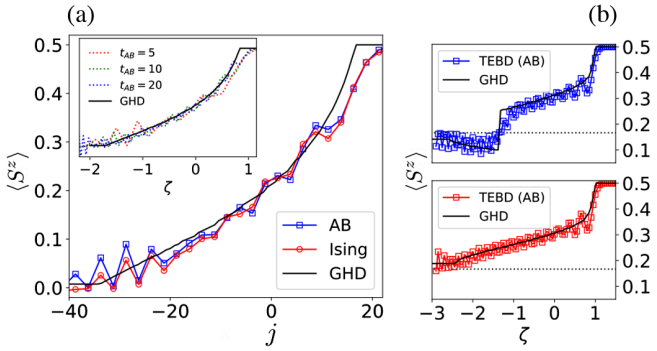

FIG. 2. (a) The magnetization profile of a chain of length $L = 80$ evolved with TEBD from $|\mathrm{Neel}\rangle \otimes |\mathrm{ferro}\rangle$ at large time (measured in the AB units $[\mathcal{J}^{-1}]$) $t_{\mathrm{AB}} = 20$ approaches the GHD prediction. For the Ising model we choose parameters $h_\perp = 0.5$, $h_\parallel = 6$, and $J = 1$, corresponding to $\Delta = 0.5$ in the AB model. In the inset, we show the collapse of the AB simulations on the GHD analytical prediction. (b) To highlight magnetization jumps in $|\Delta| > 1$ (precisely, $\Delta = 1.5, \mathcal{J} = -1$), we consider the partitioning from $|\mathrm{GS}_{\langle Z\rangle}\rangle \otimes |\mathrm{ferro}\rangle$ with $|\mathrm{GS}_{\langle Z\rangle}\rangle$ the ground state of the AB model in the sector at fixed magnetization $\langle Z\rangle$ for a chain of length $L = 120$. For the left-side magnetization being below (top) and above (bottom) the half filling dotted line, the profile exhibits qualitatively different behavior.

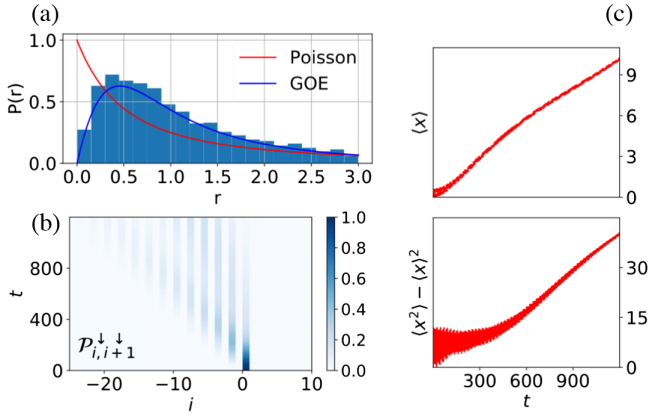

FIG. 3. (a) The level statistics analysis shows compatibility with the Gaussian orthongonal ensemble [49], suggesting that the sector with a two-magnon cluster is not integrable. The distribution function $P(r)$ is defined in the Supplemental Material [61] and computed with the exact diagonalization package QuSpin [83,84]. (b) A two-magnon cluster, initially at the center of a chain of length $L = 80$ bipartitioned into antiferromagnetic and ferromagnetic halves, can move to the left by virtue of the magnon-assisted hopping. We track its position by measuring the projector on two consecutive flipped spins $\mathcal{P}^{\downarrow\downarrow}_{i,i+1}$. (c) At large times, the position $\langle x\rangle$ and variance $\langle x^2\rangle - \langle x\rangle^2$ of the cluster evolve linearly in time, as described in the main text. The TEBD simulations for (b) and (c) are done with the Ising Hamiltonian with parameters corresponding to $\Delta = 0.5$ and $\mathcal{J} = -1$.

Gaussian orthogonal random matrix ensemble; see Fig. 3(a) and the Supplemental Material [61] for a detailed analysis. As mentioned before, within leading order perturbation theory clusters are frozen when isolated [82] and do not contribute to transport by themselves, but their mobility is activated by the scattering with a magnon. If the scattering is reflective, the cluster stands still, but if transmission occurs the cluster hops by two sites in the direction opposite to the traveling magnon. Therefore, one can relate the cluster displacement x with the total magnetization transported through it as $x = 2\delta S^z$. Given that, the cluster position reflects the local transport of spin and its fluctuations. At late times, a cluster of two magnons undergoes a biased random walk, hopping in the left and right directions with certain rates $R_{L,R}$ which depend on the interactions with the magnonic gas and being proportional to its density. Hence, at a late time the cluster experiences diffusion [61] with a linear growth of the average position and variance; see Fig. 3.

Conclusions and outlook.—We discussed the rich phenomenology and transport in the weakly tilted Ising spin chain, exhibiting fragmentation, emergent integrability, and magnon-assisted cluster dynamics. Rydberg atoms in optical tweezers could be used to probe the slow exotic physics of magnons and clusters discussed here. This experimental platform provides a versatile tool for studying many-body quantum dynamics of Ising-type models in a tilted field [85–87]. The ability to tune the model parameters and the unprecedented control of the initial state [88] opens a pathway toward experimental investigation of the constrained integrable dynamics emerging in the Ising model in a weak transverse field. In particular, the latter can be seen as a quantum simulator of the Alcaraz Bariev model with completely tunable interaction. Finally, interesting questions concerning the role of a finite density of integrability-breaking clusters on the late time thermalization and transport remain open for future investigations.

We acknowledge useful discussions with Bruno Bertini, Tom Iadecola, Alessio Lerose, and Yuan Miao. We thank Bhilahari Jeevanesan for help with the exact diagonalization study of Hilbert space fragmentation. The work of U. B. and S. M. is supported by the Emmy Noether Programme of German Research Foundation (DFG) under Grant No. MO 3013/1-1. S. M. is also supported by Vetenskapsrådet (Grant No. 2021-03685). A. B. acknowledges support from the Deutsche Forschungsgemeinschaft (DFG, German Research Foundation) under Germany's Excellence Strategy EXC2111390814868.

[1] L. Onsager, Phys. Rev. **65**, 117 (1944).
[2] P. Calabrese, F. H. L. Essler, and M. Fagotti, Phys. Rev. Lett. **106**, 227203 (2011).
[3] P. Calabrese, F. H. L. Essler, and M. Fagotti, J. Stat. Mech. (2012) P07016.
[4] P. Calabrese, F. H. L. Essler, and M. Fagotti, J. Stat. Mech. (2012) P07022.
[5] T. D. Schultz, D. C. Mattis, and E. H. Lieb, Rev. Mod. Phys. **36**, 856 (1964).
[6] B. M. McCoy and T. T. Wu, Phys. Rev. D **18**, 1259 (1978).
[7] G. Delfino, G. Mussardo, and P. Simonetti, Nucl. Phys. **B473**, 469 (1996).
[8] S. B. Rutkevich, J. Stat. Phys. **131**, 917 (2008).
[9] P. Fonseca and A. Zamolodchikov, J. Stat. Phys. **110**, 527 (2003).
[10] M. Kormos, M. Collura, G. Takács, and P. Calabrese, Nat. Phys. **13**, 246 (2017).
[11] P. P. Mazza, G. Perfetto, A. Lerose, M. Collura, and A. Gambassi, Phys. Rev. B **99**, 180302(R) (2019).
[12] R. Verdel, F. Liu, S. Whitsitt, A. V. Gorshkov, and M. Heyl, Phys. Rev. B **102**, 014308 (2020).
[13] A. Lerose, F. M. Surace, P. P. Mazza, G. Perfetto, M. Collura, and A. Gambassi, Phys. Rev. B **102**, 041118(R) (2020).
[14] J. Vovrosh and J. Knolle, Sci. Rep. **11**, 11577 (2021).
[15] O. A. Castro-Alvaredo, M. Lencsés, I. M. Szécsényi, and J. Viti, Phys. Rev. Lett. **124**, 230601 (2020).
[16] A. J. A. James, R. M. Konik, and N. J. Robinson, Phys. Rev. Lett. **122**, 130603 (2019).
[17] N. J. Robinson, A. J. A. James, and R. M. Konik, Phys. Rev. B **99**, 195108 (2019).
[18] W. D. Roeck and V. Verreet, arXiv:1911.01998.
[19] S. Pai and M. Pretko, Phys. Rev. Research **2**, 013094 (2020).

[20] F. M. Surace and A. Lerose, New J. Phys. **23**, 062001 (2021).
[21] P. I. Karpov, G. Y. Zhu, M. P. Heller, and M. Heyl, arXiv:2011.11624.
[22] A. Sinha, T. Chanda, and J. Dziarmaga, Phys. Rev. B **103**, L220302 (2021).
[23] G. Lagnese, F. M. Surace, M. Kormos, and P. Calabrese, Phys. Rev. B **104**, L201106 (2021).
[24] A. Milsted, J. Liu, J. Preskill, and G. Vidal, arXiv:2012.07243.
[25] M. Rigobello, S. Notarnicola, G. Magnifico, and S. Montangero, Phys. Rev. D **104**, 114501 (2021).
[26] R. J. V. Tortora, P. Calabrese, and M. Collura, Europhys. Lett. **132**, 50001 (2020).
[27] O. Pomponio, M. A. Werner, G. Zarand, and G. Takacs, SciPost Phys. **12**, 61 (2022).
[28] S. Jiang and O. Motrunich, Phys. Rev. B **99**, 075103 (2019).
[29] U. Borla, R. Verresen, J. Shah, and S. Moroz, SciPost Phys. **10**, 148 (2021).
[30] D. Bernard and B. Doyon, J. Stat. Mech. (2016) 064005.
[31] F. C. Alcaraz and R. Z. Bariev, arXiv:cond-mat/9904042.
[32] I. N. Karnaukhov and A. A. Ovchinnikov, Europhys. Lett. **57**, 540 (2002).
[33] F. C. Alcaraz and M. J. Lazo, J. Stat. Mech. (2007) P08008.
[34] R. Verresen, A. Vishwanath, and F. Pollmann, arXiv:1903.09179.
[35] U. Borla, R. Verresen, F. Grusdt, and S. Moroz, Phys. Rev. Lett. **124**, 120503 (2020).
[36] Z.-C. Yang, F. Liu, A. V. Gorshkov, and T. Iadecola, Phys. Rev. Lett. **124**, 207602 (2020).
[37] L. Zadnik and M. Fagotti, SciPost Phys. Core **4**, 10 (2021).
[38] L. Zadnik, K. Bidzhiev, and M. Fagotti, SciPost Phys. **10**, 99 (2021).
[39] B. Pozsgay, T. Gombor, A. Hutsalyuk, Y. Jiang, L. Pristyák, and E. Vernier, Phys. Rev. E **104**, 044106 (2021).
[40] P. Sala, T. Rakovszky, R. Verresen, M. Knap, and F. Pollmann, Phys. Rev. X **10**, 011047 (2020).
[41] V. Khemani, M. Hermele, and R. Nandkishore, Phys. Rev. B **101**, 174204 (2020).
[42] S. Moudgalya, A. Prem, R. Nandkishore, N. Regnault, and B. A. Bernevig, Thermalization and its absence within krylov subspaces of a constrained hamiltonian, in *Memorial Volume for Shoucheng Zhang* (2021), Chap. 7, pp. 147–209, 10.1142/9789811231711_0009.
[43] Z. Papić, arXiv:2108.03460.
[44] S. Moudgalya, B. A. Bernevig, and N. Regnault, arXiv:2109.00548.
[45] B. Pozsgay, J. Phys. A **54**, 384001 (2021).
[46] B. Pozsgay, T. Gombor, and A. Hutsalyuk, Phys. Rev. E **104**, 064124 (2021).
[47] T. Gombor and B. Pozsgay, Phys. Rev. E **104**, 054123 (2021).
[48] O. A. Castro-Alvaredo, B. Doyon, and T. Yoshimura, Phys. Rev. X **6**, 041065 (2016).
[49] B. Bertini, M. Collura, J. De Nardis, and M. Fagotti, Phys. Rev. Lett. **117**, 207201 (2016).
[50] A. Bastianello, B. Bertini, B. Doyon, and R. Vasseur, J. Stat. Mech. (2022) 014001.
[51] J. D. Nardis, B. Doyon, M. Medenjak, and M. Panfil, J. Stat. Mech. (2022) 014002.
[52] V. Alba, B. Bertini, M. Fagotti, L. Piroli, and P. Ruggiero, J. Stat. Mech. (2021) 114004.
[53] V. B. Bulchandani, S. Gopalakrishnan, and E. Ilievski, J. Stat. Mech. (2021) 084001.
[54] A. Bastianello, A. D. Luca, and R. Vasseur, J. Stat. Mech. (2021) 114003.
[55] M. Borsi, B. Pozsgay, and L. Pristyák, J. Stat. Mech. (2021) 094001.
[56] A. C. Cubero, T. Yoshimura, and H. Spohn, J. Stat. Mech. (2021) 114002.
[57] L. Piroli, J. De Nardis, M. Collura, B. Bertini, and M. Fagotti, Phys. Rev. B **96**, 115124 (2017).
[58] U. Schollwck, Ann. Phys. (Amsterdam) **326**, 96 (2011), january 2011 Special Issue.
[59] J. R. Schrieffer and P. A. Wolff, Phys. Rev. **149**, 491 (1966).
[60] S. Bravyi, D. P. DiVincenzo, and D. Loss, Ann. Phys. (Amsterdam) **326**, 2793 (2011).
[61] See Supplemental Material at http://link.aps.org/supplemental/10.1103/PhysRevLett.128.196601 for construction of the effective Hamiltonian; integrability and hydrodynamics of the Alcaraz-Bariev model; analysis of the energy level statistics; dynamics of a two-magnon cluster.
[62] C.-J. Lin and O. I. Motrunich, Phys. Rev. A **95**, 023621 (2017).
[63] P. Fendley, K. Schoutens, and J. de Boer, Phys. Rev. Lett. **90**, 120402 (2003).
[64] P. Fendley, B. Nienhuis, and K. Schoutens, J. Phys. A **36**, 12399 (2003).
[65] J. Minar, B. van Voorden, and K. Schoutens, arXiv:2005.00607.
[66] E. Ilievski, M. Medenjak, T. Prosen, and L. Zadnik, J. Stat. Mech. (2016) 064008.
[67] M. Rigol, V. Dunjko, V. Yurovsky, and M. Olshanii, Phys. Rev. Lett. **98**, 050405 (2007).
[68] A. B. Zamolodchikov, arXiv:hep-th/0401146.
[69] Y. Jiang, arXiv:2011.00637.
[70] J. Cardy and B. Doyon, J. High Energy Phys. 04 (2022) 136.
[71] B. Doyon, J. Durnin, and T. Yoshimura, arXiv:2105.03326.
[72] M. Medenjak, G. Policastro, and T. Yoshimura, Phys. Rev. D **103**, 066012 (2021).
[73] E. Marchetto, A. Sfondrini, and Z. Yang, Phys. Rev. Lett. **124**, 100601 (2020).
[74] B. Pozsgay, Y. Jiang, and G. Takács, J. High Energy Phys. 03 (2020) 092.
[75] M. Takahashi, *Thermodynamics of One-Dimensional Solvable Models* (Cambridge University Press, Cambridge, England, 2005).
[76] J.-S. Caux and F. H. L. Essler, Phys. Rev. Lett. **110**, 257203 (2013).
[77] J.-S. Caux, J. Stat. Mech. (2016) 064006.
[78] M. Borsi, B. Pozsgay, and L. Pristyák, Phys. Rev. X **10**, 011054 (2020).
[79] B. Pozsgay, Phys. Rev. Lett. **125**, 070602 (2020).
[80] V. Oganesyan and D. A. Huse, Phys. Rev. B **75**, 155111 (2007).
[81] Y. Y. Atas, E. Bogomolny, O. Giraud, and G. Roux, Phys. Rev. Lett. **110**, 084101 (2013).
[82] The hopping of an isolated cluster composed of ℓ magnons scales $\sim h_{\perp}^{2\ell}$.
[83] P. Weinberg and M. Bukov, SciPost Phys. **2**, 003 (2017).

[84] P. Weinberg and M. Bukov, SciPost Phys. **7**, 20 (2019).
[85] H. Bernien, S. Schwartz, A. Keesling, H. Levine, A. Omran, H. Pichler, S. Choi, A. S. Zibrov, M. Endres, M. Greiner, V. Vuletić, and M. D. Lukin, Nature (London) **551**, 579 (2017).
[86] J. Zeiher, J.-y. Choi, A. Rubio-Abadal, T. Pohl, R. van Bijnen, I. Bloch, and C. Gross, Phys. Rev. X **7**, 041063 (2017).
[87] V. Lienhard, S. de Léséleuc, D. Barredo, T. Lahaye, A. Browaeys, M. Schuler, L.-P. Henry, and A. M. Läuchli, Phys. Rev. X **8**, 021070 (2018).
[88] A. Browaeys and T. Lahaye, Nat. Phys. **16**, 132 (2020).